Novel Amphiphilic Hyperbranched Poly (amine-ester) Copolymers Nanoparticles as Protein Drug Delivery

Ming Jiang[1,2], Tiewei Wang[1], Qing Xu[1] and Yan Wu[1,*]

[1]*National Center for Nanoscience and Technology, China, Beijing 100190, China;* [2]*State Key Laboratory of Chemical Resource Engineering Key Lab of Beijing City on Preparation and Processing of Novel Polymer Materials, Beijing University of Chemical Technology, China, Beijing 100029, China*

Abstract: Novel amphiphilic protein-loaded hyperbranched poly (amine-ester) copolymers nanoparticles were fabricated by double emulsion (DE) and nanoprecipitation (NP) methods. Encapsulation efficiency (EE) of nanoparticles to Bovine serum albumin (BSA) could reach 97.8% at BSA (0.01g/ml), internal phase volume (0.5ml), copolymer weight (50mg), and PVA concentration (4%, w/v) condition.

Key Words: Hyperbranched poly (amine-ester), poly(lactide), ring-opening polymerization, nanoaprticles, double emulsion (DE) method, nanoprecipitation (NP) method, bovine serum albumin, protein delivery system.

1. INTRODUCTION

In recent years, the strategy of utilizing the polymeric micelles as a carrier system for delivery of drugs has gained increasing interest. Polymeric micelles prepared from amphiphilic block copolymers such as PLA /PEG (poly (ethylene glycol)), PLGA (poly (D, L-lactide -co-glycolide))/PEG possess a nano-scale size range, these nanoparticles NPs) are conjugated or interacted with a therapeutic agent of interest within their polymeric matrix or onto the surface, and the NPs with hydrophobic surface were easily adsorbed by protein and phagocytosed by cells of the reticuloeddothelial system (RES) [1-7]. Polymeric micelles as novel drug vehicles present numerous advantages, such as reduced side effects of anticancer drugs and selective targeting, it also allows for controlling the release pattern of drug and sustaining drug levels for a long time by appropriately selecting the polymeric carrier.

Dendritic polymers including dendrimers and hyperbranched polymers have a highly branched structure, intramolecular voids, small rheological volumes, lower viscosity in solution, providing a high density of functional groups at the periphery [8-10]. It is also suitable for a wide range of biomedical applications including drug delivery, detoxication, microarray systems and catalysis [11-13]. Dendrimers which may have more defined and ordered branching structure have to be obtained step by step with time-consuming and expensive synthetic and purification procedures [14,15]. In comparison, hyperbranched polymer, which has similar figuration as dendrimer and was synthesized much easier than dendrimer, may be a new type of potential application for the drug delivery system [16,17]. Hyperbranched polymers contain numerous end-groups in their molecular structures and the characteristics of these terminal groups have a great influence on the properties of resulting hyperbranched polymers. Therefore, modification of the number and type of end-groups is a powerful tool to tailor the properties of hyperbranched polymers [18].

In this paper, the hyperbranched polymers contain repeating internal tertiary amine-linkage and abundant surface hydroxyl groups that enable further modification. The polymers were then designed to introduce the PLA by modification of the surface hydroxyl groups of the product. The copolymers were characterized on the basis of ^{1}H NMR, ^{13}C NMR and FT-IR measurements. The morphological examination of nanoparticles was performed using a transmission electron microscope (TEM) for morphology analysis, encapsulation efficiency, release profiles and stability of BSA released from the NPs were also investigated.

2. EXPERIMENTAL SECTION

2.1. Materials

1, 1, 1-trimethylol propane of reagent grade, methyl acrylate purified by vacuum distillation and diethanolamine were purchased from National Medicines chemical Reagent Co. Ltd (China.), titanium tetraisopropoxide ($Ti(OiPr)_4$), benzoic anhydride and imidazole were purchased from Beijing Reagent Factory,(China), D, L-lactide (DLLA) was obtained from (Alfa Aesar, America), $Sn(Oct)_2$ was purchased from Sigma (America), Poly(vinyl alcohol) (PVA) was purchased from Guangdong, XILONG Chemical Industry Co, Ltd. (China.), BSA (MW=66 kDa) was purchased from Sigma (St. Louis, MO). BCA protein assay kit was purchased from Beyotime Institute of Biotechnology (China). All other reagents and solvents were of analytical grade.

2.2. Synthesis and Characterization of HPAE-co-PLA Copolymer

2.2.1. Synthesis HPAE-OHs

HPAE–OHs were synthesized through a pseudo-one-step process [19, 20] with few modifications by alcoholysis at

*Address correspondence to this author at the National Center for Nanoscience and Technology, China, Beijing 100190, China;
Tel: +86 10 82545614; Fax: +86 10 62656765; E-mail: wuy@nanoctr.cn

1389-5575/09 $55.00+.00

120°C using 1, 1, 1-trimethylol propane (as a molecular core) and N, N-diethylol-3-amine methylpropionate (as an AB_2 monomer) with $Ti(OiPr)_4$ as the catalyst. The generation of HPAE-OHs was increased by repeatedly adding N, N-diethylol-3-amine methylpropionate monomer to the former generation product. The fourth-generation HPAE-OHs4 was obtained by repeating the process three times. The product was dissolved in 10 ml ethanol, and the $Ti(OiPr)_4$ produced the precipitate in ethanol. Then, the $Ti(OiPr)_4$ was removed by filtration. Finally the ethanol was evaporated and the product were dried at 40°C in a vacuum oven and stored for further utilization. N, N-diethylol-3-amine methylpropionate was prepared by using methyl acrylate and diethanolamine, the feed molar ratio is 1.5:1. After the Michael Reaction, excess methyl acrylate and methanol was removed by vacuum distillation.

2.2.2. Synthesis of HPAE–co- PLA Copolymer

HPAE–co-PLA copolymer (in the molar ratio of 3:1, 7:1 and 10:1, respectively (DLLA/HPAE–OHs4)) was synthesized utilizing a ring-opening polymerization procedure. D, L-lactide (DLLA) and HPAE-OHs4 were dehydrated by using P_2O_5 under vacuum at 45°C for 24 h and were used without further purification. HPAE-OHs4 was put into a glass ampoule with predetermined amounts of D, L-lactide. ($Sn(Oct)_2$) was added at about 0.1 (w/w) %. The ampoule was evacuated by a vacuum pump at 30 °C for 1 h and then sealed. The ampoule was heated in an oil bath at 140°C for 13 h. After 13 h, the reaction product was cooled to ambient temperature. The obtained viscous material was dissolved with CH_2Cl_2 and then precipitated with petroleum, and washed further by petroleum for three times to remove unreacted DL-lactide monomers. After the petroleum was evaporated, the polymers were dissolved in a little of acetone and then precipitated in deionized water. The purified polymers were dried at 25 °C for 2 days in a vacuum oven.

2.2.3. Preparation of PLA

PLA was prepared at 125 °C for 10 h by the ring opening polymerization of D,L-lactide sealed in an ampoule in the presence of $Sn(Oct)_2$ as described previously [21]. The product was purified by the repeat dissolution in chloroform and precipitation in cold methanol and was finally dried for 48 h at 40°C in a vacuum oven. The molecular weights were measured by gel permeation chromatography (GPC).

2.3. Determination the Hydroxyl Values of HPAE–OHs

The hydroxyl values of HPAE–OHs were determined by the following method [22]. HPAE-OHs was dissolved in excess benzoic anhydride with imidazole as a catalyst (in pyridine) at 80°C of water bath for three hours to acetylate the hydroxyl groups in HPAE-OHs. By back-titrating the above mixture with NaOH solution ($0.1 molL^{-1}$, in water) at room temperature, the hydroxyl values of HPAE-OHs were calculated.

2.4. Determination of the Chemical Structure of HPAE–OHs and HPAE-co-PLA Copolymer

FT-IR spectra of HPAE–OHs and HPAE-co-PLA was obtained using a (Spectrum One, Perkin-Elmer, America) spectrophotometer. The spectra of HPAE–OHs were obtained by using KBr film as a reference. The HPAE-co-PLA samples were mixed with KBr and then pressed to a plate for measurement.

The ^1H NMR spectra of HPAE-OHs and HPAE-co-PLA was recorded on a (Bruker AVANCE 400) NMR spectrometer. ^1H NMR HPAE-OHs was dissolved in $(CD_3)_2SO$. HPAE-co-PLA copolymers were dissolved in $CDCl_3$.

The ^{13}C NMR spectra of HPAE-OHs and HPAE- co-PLA was recorded on a (Bruker AVANCE 400) NMR spectrometer. ^{13}C NMR HPAE-OHs was dissolved in $(CD_3)_2SO$. HPAE-co-PLA copolymers were dissolved in $CDCl_3$.

2.5. Determination of Molecular Weight

Gel permeation chromatography (GPC) was performed on a Waters 2410 GPC apparatus (USA). Molecular weight and molecular weight distribution of the copolymer were calculated using polystyrene as the standard.

2.6. Determination of the Thermal Stability

The thermal stability of HPAE-co-PLA and PLA samples were measured by TGA (Perkin-Elmer, America). The temperature range was from 25 °C to 500 °C under nitrogen flow and the heating rate was 20°C /min.

2.7. Biodegradation of the Copolymer HPAE-co-PLA

A sample of the copolymer in weight of 20 mg was compressed in a mold into a disc in the diameter of 10 mm and in thickness of 0.3 mm on a Carver Laboratory Press (Fred S. Carver Inc., USA) at room temperature. The disc as mentioned above was incubated in PBS (pH 7.4) at 37 °C for 20 days. The weight of dried disc was measured. At the day 1, 7, 10, 15, and 20, the disc was washed with pure water thrice and dried in vacuo to a constant weight and the weight was measured. The biodegradation rate was estimated by retained weight in percentage (%).

2.8. Preparation of HPAE- co-PLA Copolymer Nanoparticles

Double emulsion (DE) method was used to fabricate nanoparticles as described by Rodrigues *et al*. [23] with some modifications. Briefly, 0.2 -2 ml BSA solution with 2 -20 mg/ml concentration was emulsified in 1-5 ml of DCM (dichloromethane) containing HPAE-PLA (20-100 mg) by homogenization at 5000 rpm in an ice bath for 3×10 s (Bailing, Model DS-200, China), a W_1/O emulsion was formed. Thereafter, this first emulsion was poured into 5-50 ml of the PVA aqueous solution (0.3-5% w/v) and homogenized at 10 000 rpm in an ice bath for 3×15 s (Bailing Model DS-200, China). The double emulsion ($W_1/O/W_2$) was diluted in 100-150 ml PVA solution (0.3%, w/v) and the DCM was rapidly eliminated by evaporation under reduced pressure. Finally, the nanoparticles were collected by centrifugation at 25 000×*g* for 25 min at 4°C (Beckman Model J2-21) and washed twice with water. The nanoparticles were diluted with 2mL of 5% glucose and stored at 4°C.

A nanoprecipitation (NP) technique [24] was developed for comparison with the DE method. Briefly, 1-5 mL of the polymer solution (10-100 mg/mL) in acetone was added dropwise to 1-20 mL of water with BSA (1-100mg) or with-

out BSA at a rate of 0.5 mL/min using a syringe pump (74,900 series multichannel syringe pumps, Cole-Parmer Instrument Company, China) under magnetic stirring. Acetone was eliminated by evaporation under reduced pressure. The nanoparticles were recovered by ultracentrifugation and treated as above in the DE method.

The effects of copolymer composition and the preparation conditions, such as BSA concentration in water phase and copolymer concentration in organic phase, on the particle size and encapsulation efficiency (EE) were evaluated.

2.9. Characterizations of the HPAE-co-PLA Copolymer NPs

2.9.1. DSC Measurement of NPs

The thermo-properties of the NPs with or without BSA, from the NP method, were investigated, and HPAE-co-PLA 7:1(molar ratio) and PLA were taken as an example. Samples (3–5 mg) were loaded into aluminum pans and the DSC thermo grams were recorded on a Pyris Diamond DSC apparatus (Perkin-Elmer, America). In order to observe Tg, all of the DSC thermo grams were obtained from a second heating procedure. Briefly, the heating rate was 20°C/min in the range of 20–100°C by using nitrogen flowing, samples were stored at 100°C for 1 min and then cooled to -50°C, the cooling rate was 20°C/min, then the samples were re-heated from 0°C to 100°C in the heating rate of 20°C/min.

2.9.2. TEM Observation

The morphological examination of nanoparticles was performed using a transmission electron microscope (TEM, JEM-200CX) following negative staining with sodium phosphotung state solution (2%, w/w).

2.9.3. Measurements of Particle Size and ζ Potential

Nanoparticle sizes and ζ potential were determined using a Zetasizer Nano series ZEN 3600 (Malvern Instruments Ltd., England). The experiment was performed at a wavelength of 633 nm with a constant angle of 90°at 25°C using the samples appropriately diluted with distilled water. For ζ potential, the sample was diluted with a 0.05 M NaCl solution to a constant ionic strength.

2.9.4. Measurements of EE

The encapsulation efficiency (EE) was determined by measuring the BSA concentration in the supernatant. The amount of non-entrapped BSA in aqueous phase was determined by the BCA protein assay in the supernatant obtained after ultracentrifugation of nanoparticles. The UV–visible spectroscopy measurements were carried out for known concentrations of BSA by using the BCA protein assay kit at the absorbance maximum of 562 nm. The EE was calculated as following equation:

$$EE\%=100\% (W_o-W_t) /W_o$$

W_o and W_t are the weight of initial BSA and that of the total amount of protein detected in supernatant after the twice centrifugation, respectively. Each sample was assayed in triplicate.

2.9.5. In Vitro Release

The NPs loading BSA were incubated in a capped centrifugal tube containing 8mL of PBS (pH 7.4), and the centrifugal tube was kept at 37 °C water baht and shaken at 120 rpm. At appropriate intervals (0.5h, 1h, 2h,3h, 4h, 5h, 6h, 7h, 8h, 1d, 3d, 5d, 6d, 7d, 10d, 14d, 21d, 28d), 1 mL of the supernatant was extracted and equal amount of fresh PBS was added to the tube, the samples were centrifuged at 13000 rpm for 10 min. BSA concentration in the supernatant was determined as described in above. Each experiment was repeated thrice and the result was the mean value of three samples. The error bars in the plot showed the standard deviation of data.

2.9.6. Stability of BSA Released from NPs

The free BSA in the supernatant after its release of 14, 28 days from the HPAE-co-PLA nanoparticles was stored at -20^{o}C. The integrity (the soluble-aggregation and degradation) of BSA was determined by sodium dodecyl sulfate polyacrylamide gel electrophoresis (SDSPAGE). The BSA in supernatant and contrast SDSPAGE analysis were performed under nonreducing conditions using a Bio-Rad electrophoresis system.

The secondary structure of released BSA and BSA control was determined by measuring circular dichroism spectra. The secondary structure was studied by CD spectra which was taken with a (Jasco J810) automatic recording spectropolarimeter at 25^{o}C and 1 cm path length from 200-300 nm under nitrogen flow. Scan rates of 500 nm/min was used with a response time of 4 s. The CD response obtained was expressed in terms of ellipticity.

The fluorescence spectra was further used to determine the tertiary structure of BSA released from NPs. Excitation was carried out at 285 nm, and emission spectra were recorded ranging from 300 to 440 nm. The excitation and emission bandwidths were 3 nm.

3. RESULTS AND DISCUSSION

3.1. Synthesis and Characterization of Hydroxyl-Terminated Hyperbranched Poly (amine-ester)s (HPAE-OHs) and Conjugation of HPAE-OHs with PLA (HPAE–co-PLA)

3.1.1. Synthesis of HPAE-OHs and HPAE -co-PLA

In our work, a fourth generation HPAE-OHs4 with surface hydroxyl groups was prepared according to the previous paper [19] with few modifications. The synthesis route is shown in Scheme (**1A**). In order to minimize the side reactions between the AB_2 monomer, the choice of effectively-available transesterification catalysts which show the best compromise between chemioselecivity and activity has attracted growing attention in chemical reactions. It showed that titanates and zirconates were the most interesting catalysts [25]. Because of above reasons, p-methylbenzene sulfonic acid (p-TsOH) was replaced by $Ti(OiPr)_4$. The final products of HPAE-OHs4 have good solubility in water, ethanol and N, N-Dimethylformamide (DMF). HPAE-co-PLA block copolymer was synthesized by a ring-opening polymerization. Mw of HPAE-PLA copolymer increased

with the molar feed ratio of the monomer D, L-lactide to HPAE. The polymerization route was shown in Scheme (**1B**). The solubility of HPAE-co-PLA was totally opposite to HPAE-OHs4, which could be solved in acetone, dichloromethane and tetrahydrofuran (THF). It indicated that PLA was conjugated to the HPAE-OHs4. The different samples named HPAE–co-PLA 3:1(feed ratio of D, L-lactide with HPAE-OHs4), HPAE-co-PLA 7:1 and HPAE–co-PLA 10:1, respectively, were synthesized.

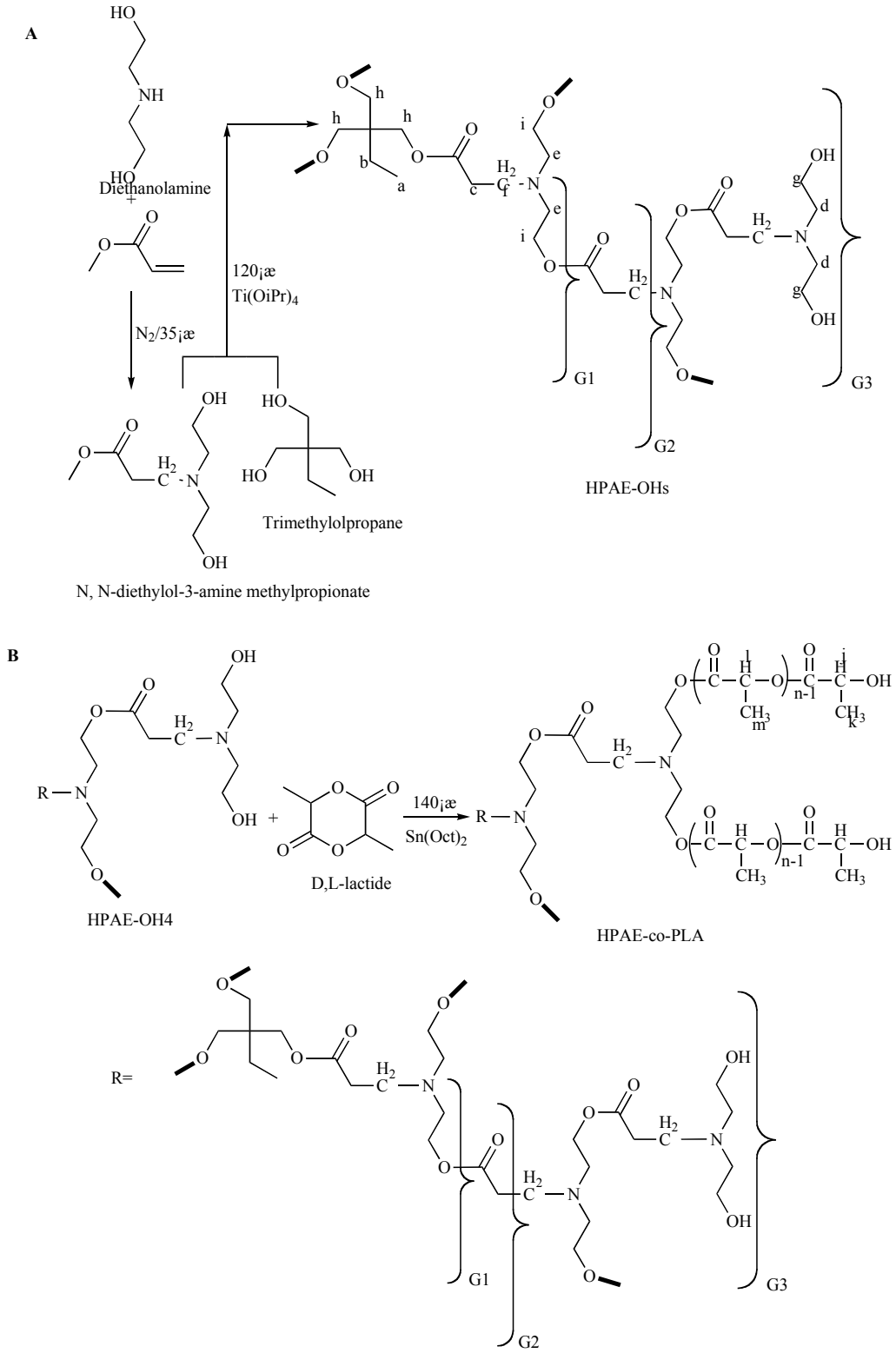

Scheme 1. (**A**) The synthesis route of HPAE-OHs. (**B**) The synthesis route of HPAE-co-PLA.

Table 1. The Hydroxyl Values of Different Generation HPAE-OHs

Hydroxyl Values of Different Generation HPAE-OHs	G2	G3	G4
Theoretical value (mgNaOH/g)	306	276	263
Experimental value (mgNaOH/g)	322	250	273

G represent the generation of HPAE-OHs.

Table 2. Composition and Molecular Weight Distribution of HPAE-co-PLA Copolymers[a]

Sample	Copolymer	Molecualr Weight of Copolymer		Polydispersity (M_w/M_n)
		M_w(kDa)	M_n(kDa)	
1	HPAE-co-PLA(3:1)	26	19	1.37
2	HPAE-co-PLA(7:1)	51	33	1.54
3	HPAE-co-PLA(10:1)	87	72	1.21

a=M_w and M_n were measured by GPC.

3.1.2. Chemical Structure of HPAE-OHs and HPAE-co-PLA

The hydroxyl values of different generation HPAE-OHs were measured and calculated by the method described in the previous paper [22]. The results of different generation HPAE-OHs were showed in the Table **1**. It could be clearly seen that with the increase of generation the hydroxyl values were close to theoretical value, which indicated that the structure was apt to regulation.

The molecular weights and polydispersity indexes of the HPAE-co-PLA copolymers were shown in Table **2**. The amount of lactide introduced to HPAE-OH4 increase with the molar ratio of DL-lactide to HPAE-OH4. When the molar ratio of lactide to HPAE-OH4 increased from 3:1 to 10:1, the molecular weights rose from 26 kDa to 87 kDa. This indicated that the higher the concentration of lactide, the higher the opportunity for the lactide to react with HPAE-OH4 reactive centers.

Fig. (**1a**,**b**) showed the infrared spectra of the HPAE-OHs4 and HPAE-co-PLA. The CH_2 scissoring and wagging modes at 1457, 1442, and 1365 cm^{-1} were different between the two graphs. For the fourth generation of HPAE-OHs4, the intensity of the three absorption bands was weak and almost equivalent. While in HPAE–co-PLA, the band located at 1454 and 1383 cm^{-1} become much stronger than the other band. The band at 1191 cm^{-1} was corresponding to the C–O stretching vibration in HPAE-OHs4 alone, while in HPAE-co-PLA the absorption intensity become stronger than HPAE-OHs4 alone. All of these changes indicated the conformational change of the HPAE-OHs4 after the conjugation to the PLA, suggesting the hydrophilic and hydrophobic interaction between HPAE-OHs4 and PLA.

The basic chemical structure of HPAE-OHs4 and HPAE–co-PLA was further confirmed by ^{1}H NMR (Fig. (**2a**,**b**)).

Compared with HPAE-OHs4 (Fig. (**2A**)), the ^{1}H NMR spectra of the HPAE–co-PLA copolymer (Fig. (**2B**)) showed that the signals at ~4.3 ppm was assigned to the terminal the methenyl protons of the branched polylactide. The signals at 1.4 and 1.5 ppm were attributed to the methyl protons of the polylactied moiety located at the terminal groups and the

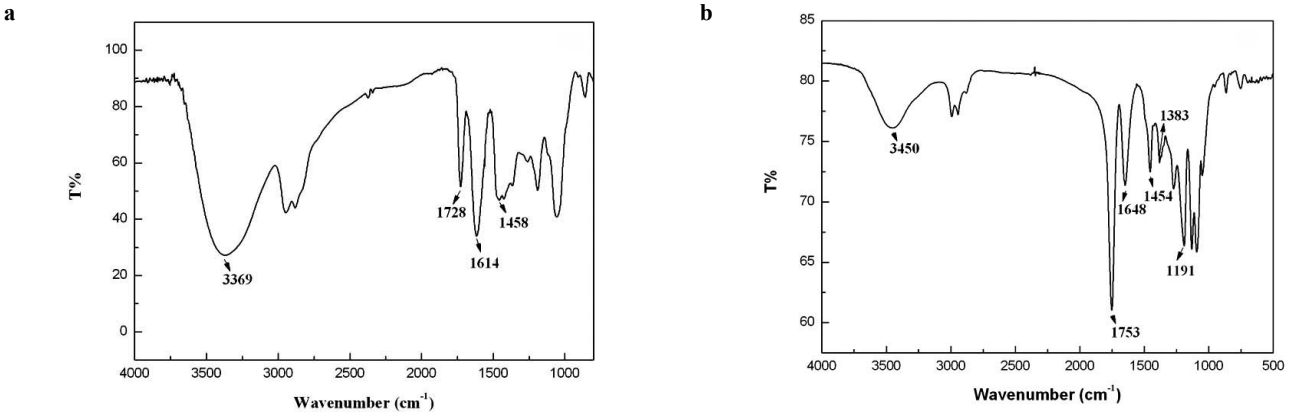

Fig. (1) . IR spectra of HPAE-OHs4 (**a**) and HPAE-co-PLA (3:1) (**b**).

A

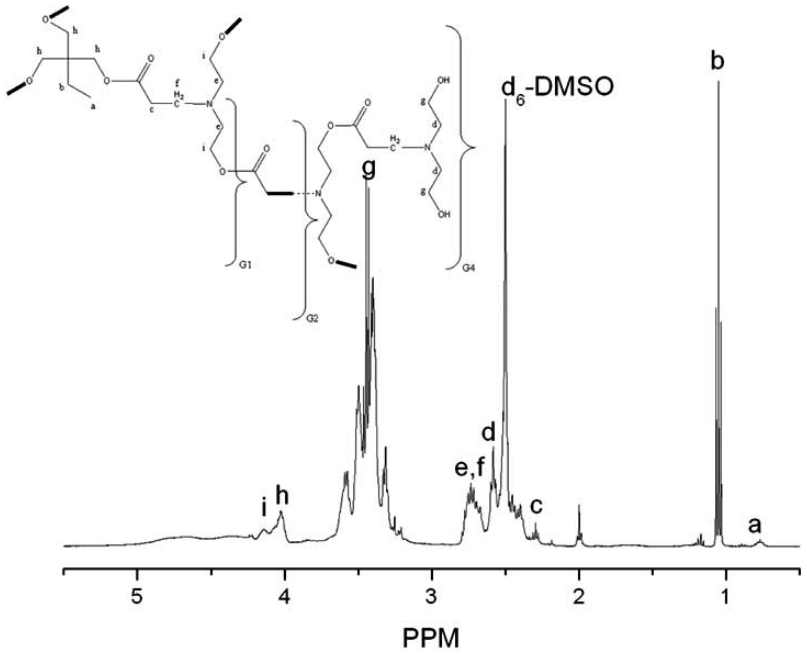
d6-DMSO
b
g
d
e,f
i
h
c
a
5
4
3
2
1
PPM

B

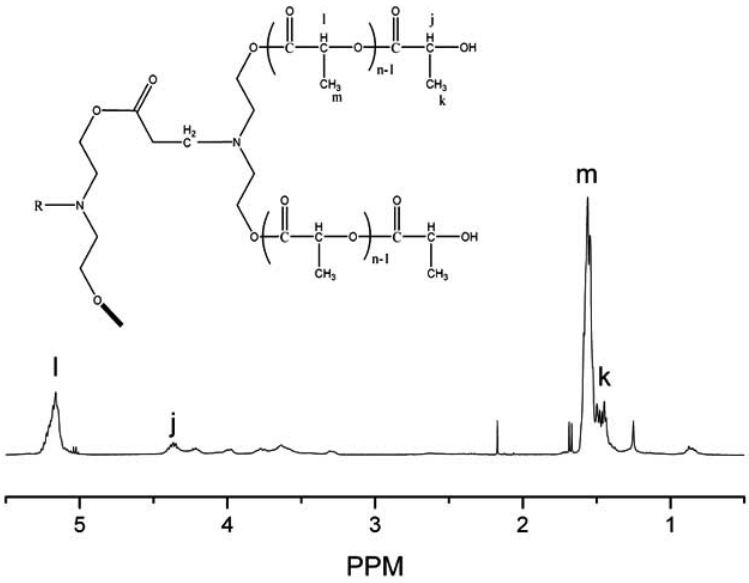
m
l
k
j
5
4
3
2
1
PPM

C

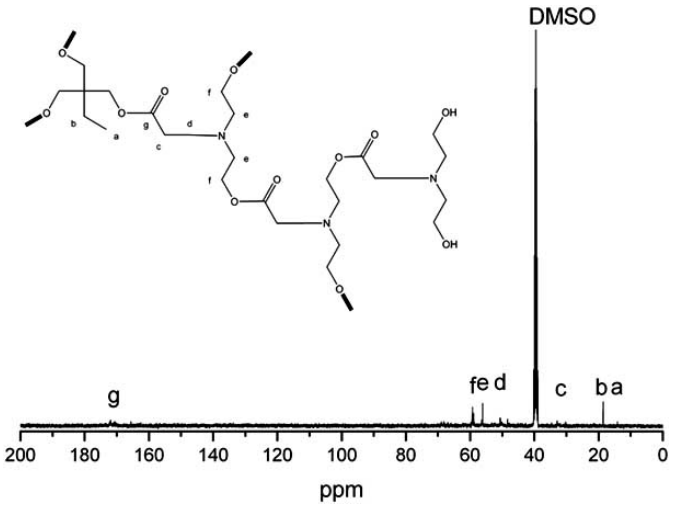
DMSO
g
fe d
c
ba
200
180
160
140
120
100
80
60
40
20
0
ppm

(Fig. 2. Contd....)

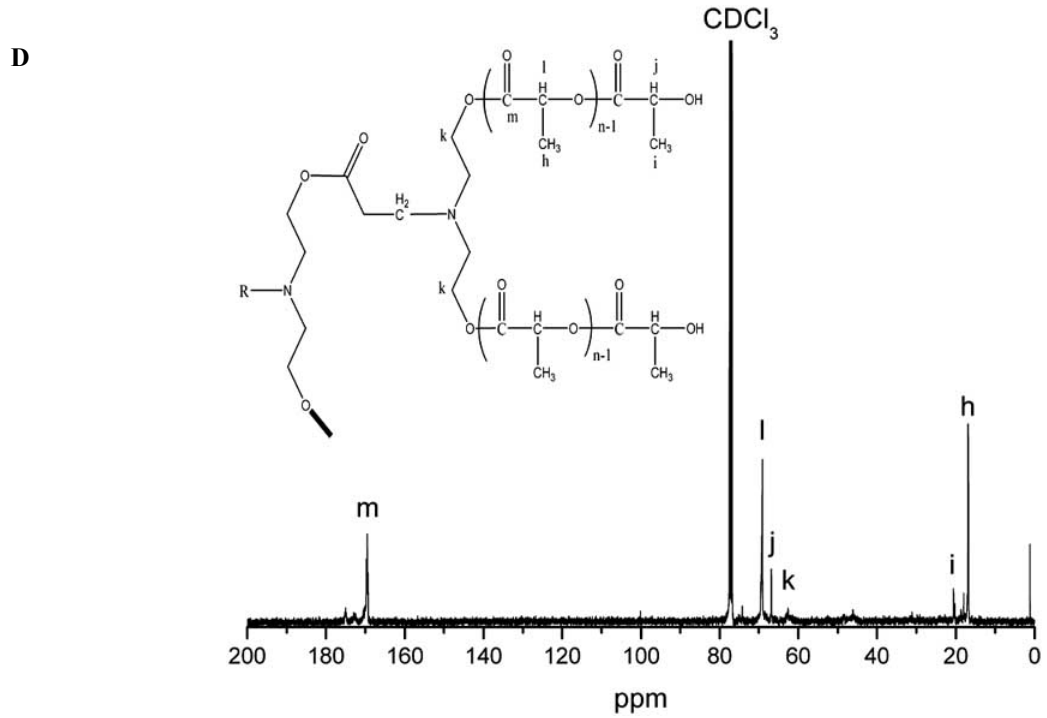

Fig. (2). ^{1}HNMR spectrum of the HPAE-OHs4 (**A**), HPAE-co-PLA (**B**) and ^{13}C NMR spectrum of the HPAE-OHs4 (**C**) and HPAE-co-PLA (**D**).

repeat units of it in the chain. All these results evidenced that the new hyperbranched copolymers contained polylactide chains.

The basic chemical structure of HPAE-OHs4 and HPAE–co-PLA were further confirmed by ^{13}CNMR, and the spectra were shown in Fig. (**2C**,**D**). Compared with HPAE-OHs4 (Fig. (**2C**)), the^{13}CNMR spectra of the HPAE–co-PLA copolymer (Fig. (**2D**)) showed that the peak at ~170 ppm was attributed to the C=O group carbon peak of polylactide. The signals at 68 and 70 ppm were assigned to CH group carbon peak of the polylactide moiety located at the terminal groups and the repeat units of it in the chain. The signals at 17 and 20 ppm were attributed to the CH_3 group carbon peak of the polylactide moiety located at the repeat units and the terminal groups. All these results evidenced that the hyperbranched copolymer contained polylactide side chains.

3.2. TGA and DSC Measurement

Fig. (**3a**) showed TGA graphs observed for HPAE-OHs4, HPAE–co-PLA and PLA samples. A fast process of weight loss appears in the TG curves response for the PLA in thermal degradation ranges. It could be seen that all of the copolymer samples exhibited a weight loss during the heating process, and the maximal weight loss rate temperature was about 210°C for all copolymer samples. The thermo decom-

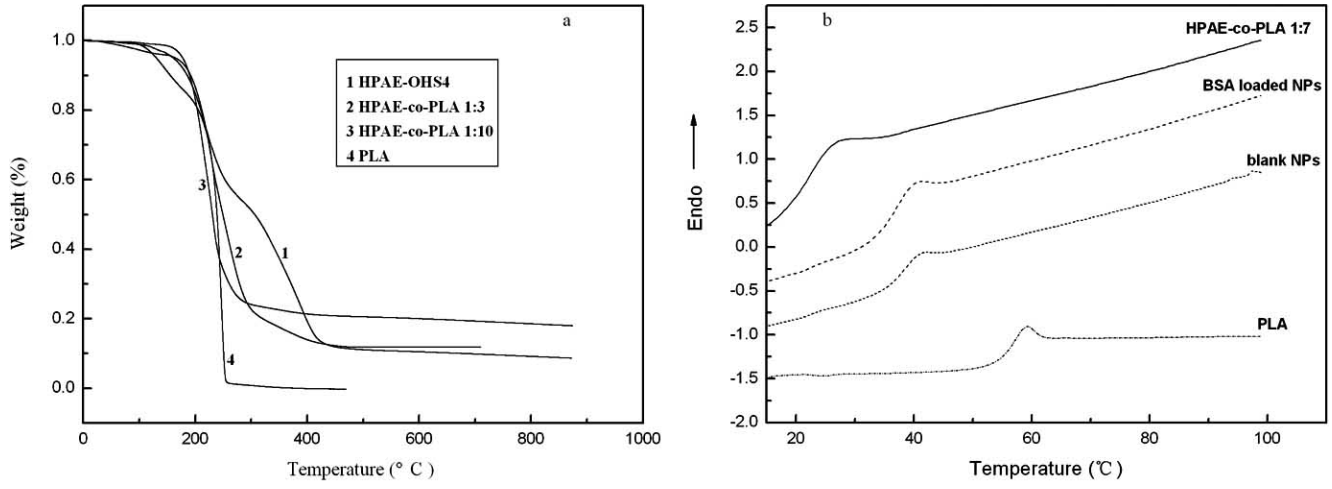

Fig. (3). TGA graphs of HPAE-OHs4, HPAE-co-PLA3:1, 10:1 and PLA (Mw=48kDa) (a) and DSC (b) thermo grams of bulk matrix, frozen blank and BSA-loaded NPs made by NP method.

posed rate and carbolic survivor increased with increase of the ratio of PLA in the copolymers. These results indicated that the thermal stability of the copolymer was decreased with increase of PLA.

In order to gain insight into the physical state of the copolymer and the NPs, The T_g of different samples were performed using DSC, and the results were shown in the Fig. (**3b**). Only one sidestep presented in all of the samples showed that there were no existence of inhomogeneities. 24.7°C could be used as the glass transition temperature of the HPAE-co-PLA which was far low compared to pure PLA after introduction PLA to HPAE-OHs4. The reason could be explained that HPAE-OHs4 with low T_g was elastic state at room temperature. The increase was observed in the T_g of blank NPs (T_g=38.0°C) compared to HPAE-co-PLA. It could be explained that some micellization behaviors of the hydrophobic and hydrophilic interaction did existed after fabrication, which influenced the three dimension structure of copolymers and made the T_g increased. Compared blank NPs and BSA loaded NPs (T_g=38.4°C), it showed that T_gs were almost the same. These results indicated that BSA had no obvious effect on the T_g during the fabrication process. The thermo properties of the NPs made by DE method were not shown here because PVA was used for stabilization and could not be washed entirely, the system was complicated for analyze.

3.3 Biodegradation of the Copolymer HPAE-co-PLA

The plots of retained weight in percentage versus time are demonstrated on Fig. (**4**). It was found that the hydrophilicity–hydrophobicity balance played an important role in the biodegradation of the HPAE-co-PLA copolymers. Since the HPAE-co-PLA copolymers were amorphous and their HPAE moieties were hydrophilic, water could be diffused into the copolymer matrix so that the biodegradation could take place simultaneously inside the copolymer disk and on its outer layer. In addition, the copolymer HPAE-co-PLA with small molecular weight was biodegraded with the higher rate than those with large molecular weight. That was because the polymeric chains of small molecular weight possessed better mobility and more hydrophilicity so that the penetration of water molecules into the polymer matrix became easy.

3.4. Preparation of BSA Loaded Copolymer NPs

3.4.1. Effect of Copolymer Composition on Particle Size and EE

The HPAE-co-PLA nanoparticles were fabricated by both DE and NP methods. Data were shown in Table **3**. In both methods, Regarding to particle size, the higher Mw of PLA contributes to the viscosity increase of copolymer solution and the decrease of HPAE-OHs4 relative contents, both factors resulting in particle size increase. The increased viscosity could decrease the diffuse of BSA, which was in favor of EE enhancing, but on the other hand, the interactions between HPAE-OHs4 and BSA may decrease with the lowering of HPAE-OHs4 relative contents, which was unfavorable for enhancing EE. For above reasons, the EE of different samples increased with the increasing of MW of PLA when the feed ratio of PLA was added from 3:1 to 7:1, but as shown in the Table **3**, EE was declined when the feed ratio of copolymer was 10:1(DLLA/ HPAE-OHs4).

The encapsulation efficiency (EE%) of BSA in the HPAE-co-PLA nanoparticles was much improved in the comparision with EE% of BSA in the corresponding PLA nanoparticles. The reasons for high EE% will be considered as follows. Firstly, Hyperbranched polymers have unique chain structure. Distinct from their linear analogues, hyperbranched polymers have structures and topologies similar to those of dendrimers, and possess some strikingly superior material properties, such as low solution/melt viscosity, enhanced solubility, abundance in terminal group, etc. Hyperbranched polymers contain numerous end-groups in their molecular structures and the characteristics of these terminal groups have a great influence on the properties of resulting hyperbranched polymers. The hyperbranched moiety was

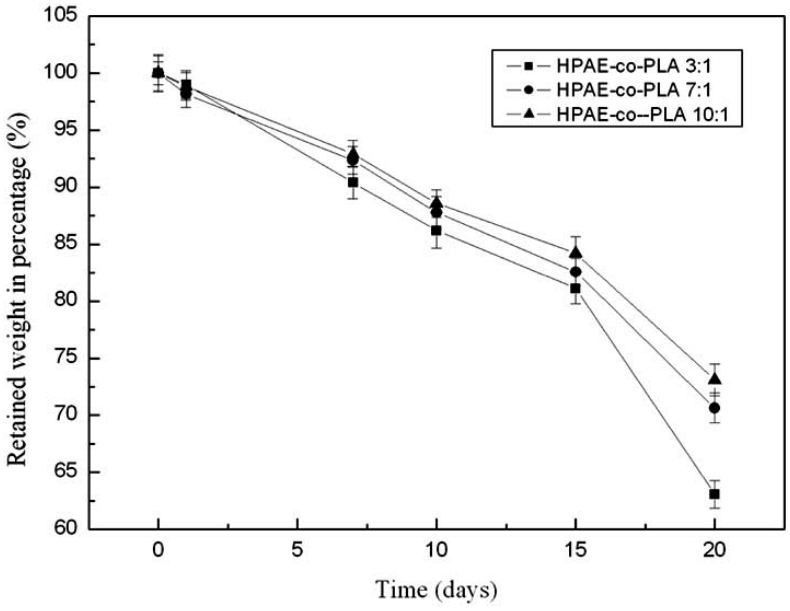

Fig. (4). Retained weight in percentage of the HPAE-co-PLA samples in PBS (pH 7.4) at 37°C.

Table 3. Effect of Material Composition on EE and Particle Size [a,b,c,d]

Method	Material Composition	EE (%)	Mean Hydrodynamic Diameter (nm)	PDI	ξ Potential (mv)
DE	3:1 (HPAE–co-PLA)	62.8 ± 2.1	142.9±1.1	0.296-0.315	-13.6±1.2
DE	7:1 (HPAE–co-PLA)	81.3 ±0.8	149.4±2.3	0.177-0.206	-22.5±1.5
DE	10:1 (HPAE–co-PLA)	51.0 ±1.3	163.4±3.8	0.129-0.231	-26.5±2.3
NP	3:1(HPAE–co-PLA)	18.6±3.2	142.3±0.9	0.124-0.166	-21.3±0.6
NP	7:1(HPAE–co-PLA)	59.8 ±2.5	146.8±1.4	0.087-0.134	-23.3±1.3
NP	10:1(HPAE–co-PLA)	36.0 ±0.6	163.2±4.3	0.120-0.145	-30.6±1.9
DE	PLA	43.6±2.2	410.2±4.6	0.152-0.224	-32.3±2.5
NP	PLA	33.7±3.1	251.8±5.4	0.206-0.246	-43.2±1.1

a. For DE method, 0.5ml BSA solution (10mg/ml) was used as inner aqueous phase. 50mg copolymer HPAE–co-PLA was dissolved in 2.5ml dichloromethane, 50mg PLA was dissolved in 3 ml dichloromethane/ acetone (1:1), PVA concentration was 3% (w/v).

b. For NP method, 5mg BSA was dissolved in 10ml water, 50mg copolymer was dissolved in 1ml acetone, 50mg PLA was dissolved in a mixture consisting of 1ml acetone and 0.05ml dichloromethane.

c. Molecular weight (Mw=48kDa) of PLA homopolymer was similar to the molecular weight of PLA in copolymer of HPAE–co-PLA (7:1).

d. PDI represents polydispersity index.

favorable for interactions between HPAE-OHs4 and BSA. Secondly, the copolymer HPAE–co-PLA was amphiphilic so that its hydrophilic part was accessible to the water-soluble BSA molecule. All the effects contributed to the increased EE%. If the HPAE-OHs moiety was helpful for the improvement of EE%, it was easy to understand why the HPAE–co-PLA copolymer could form the nanoparticles loading more BSA. Of course, the better hydrophilic/ hydrophoblic balance of the HPAE–co-PLA copolymer must be important.

ζ potential values are listed in Table **3**. The blank PLA nanoparticles had a large negative ζ potential due to the presence of the ionized carboxyl groups on the nanospheric surface. As found from the data in Table **3**, the ξ values of the HPAE-co-PLA nanoparticles were lower than those of PLA nanospheres, indicating that the HPAE-co-PLA nanoparticles possessed less negative charge because no free carboxylic group existed on the HPAE-co-PLA copolymers. The ξ potential of the nanoparticles prepared in the DE method was lower than that in the NP method since the PVA was difficult to be removed from the nanoparticle surfaces and the residue PVA could decrease the negative potential of the nanoparticles [26]. Theoretically, the nanoparticles aggregation easily occurred when ξ potential was reduced, leading to the formation of large nanoparticles [27]. However, not much aggregation was observed in our experiments. The hydrophilic HPAE moieties of the copolymer HPAE-co-PLA act as a steric barrier on the surface of the nanoparticles.

The nanoparticle EE was also influenced by the fabrication technique. In the DE method the EE were more than the NP method. This phenomenon could be interpreted in the sketch of the proposed mechanisms for the nanoparticle formations in two methods as shown in Fig. (**5**). The multi-nanoreservoir system was formed in the DE method while the single-layer nanosphere was fabricated in the NP method.

3.4.2. Effect of Fabrication Method on Particle Size and EE

3.4.2.1. DE Method

DE method was chosen as the most appropriate method because protein is highly soluble in water. The result was shown in Table **4**.

3.4.2.1.1. Effect of BSA Concentration in the Inner Aqueous Phase on Particle Size and EE

It was reported that BSA tend to accumulate at air/water, oil/water or solid/water interfaces. Therefore, the BSA could act as an excellent surfactant which was widely used to stabilize emulsions and further influence the particle size [28, 29]. It meant that with the increase of the protein concentration in the inner aqueous phase, the particle size became smaller. EE increased at first with higher protein concentration in the inner aqueous phase. EE decreased a lot when protein concentration in the inner aqueous phase was increased from 0.01 to 0.015 g/ml. The difference in osmotic pressure between the internal and external aqueous phases could be responsible for the decrease in entrapment efficiency. The osmotic pressure difference did rise with increase of BSA loading and promote an exchange between the internal and external aqueous phases, with a consequent loss of BSA [30].

3.4.2.1.2. Effect of Inner Aqueous Phase Volume on Particle Size and EE

Coalescence of droplets could be prevented by increasing internal phase. An increase in the internal aqueous phase volume of the same concentration led to a decrease of nanoparticles' average size. Since an opposite effect exists, EE showed same phenomena as mentioned in the above section. It was reported that the precipitation of the polymer solution phase was accelerated and the hardening time was shortened with the increase of inner aqueous, which was in

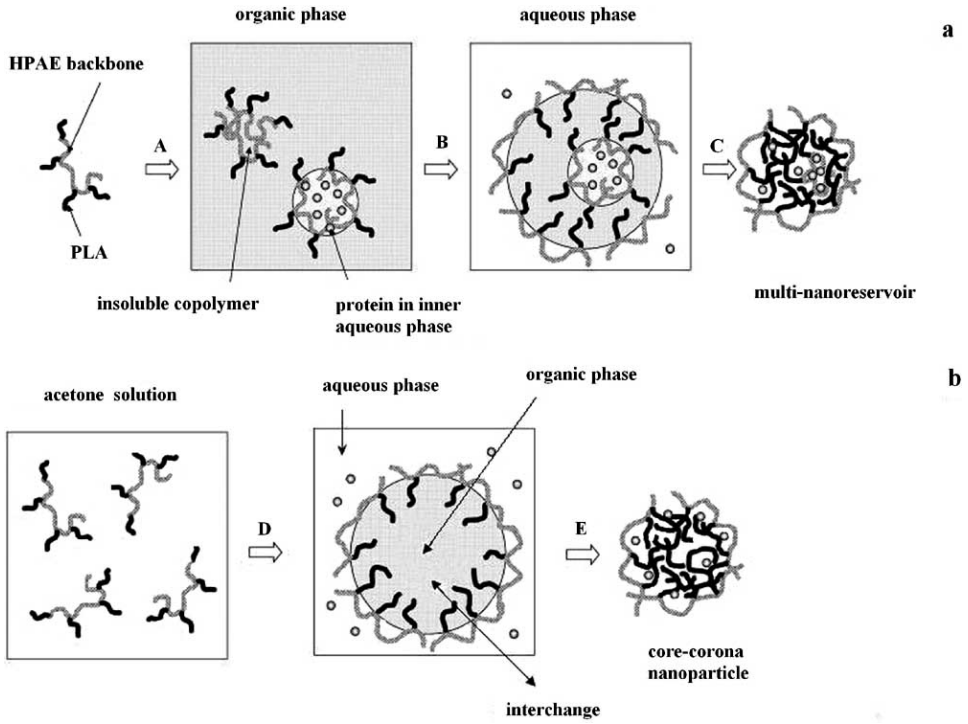

Fig. (5). Supposed mechanisms of protein encapsulation into the nanoparticles from the HPAE-co-PLA copolymer in both DE (a) and NP (b) methods. (**A**) Sonication of the HPAE-co-PLA copolymer dissolved in methylene chloride/acetone (1:1) in the presence of an aqueous protein solution led to the formation of a W_1/O emulsion. (**B**) Sonication of the W_1/O emulsion in the presence of an outer aqueous phase gave a $W_1/O/W_2$ emulsion. (**C** and **E**) The nanoparticles were formed after the solvent evaporation. (**D**) When the solution of a HPAE-co-PLA copolymer in acetone was injected into an aqueous solution of BSA, the nanoprecipitation took place.

favor of EE [29]. As mentioned in the above section, when the content of BSA was increased at a certain extent, BSA was lost from inner phase to outer phase.

3.4.2.1.3. Effect of Polymer Concentration in the Organic Phase on Particle Size and EE

Since a high viscosity hampered the shear forces of emulsion, an increase in the polymer concentration resulted in an increase of the particle mean diameter from 132.6 to 152.1 nm with a broadened particle size distribution. While the EE increased when the polymer concentration in organic phase increased since high viscosity and more HPAE-OHs4 relative contents avoided the loss of BSA.

3.4.2.1.4. Effect of PVA Concentration in the External Aqueous Phase on Particle Size and EE

An increase in external aqueous concentration of PVA from 1% to 4% (w/v) led to a decrease in particle size. The

Table 4. The Influence of Fabricating Factors on EE and Particle Size by DE Method[a,b]

No.	BSA Con. (g/ml)	Internal Phase Volume (ml)	Polymer Weight (mg)	PVA Con. (w/v %)	EE (%)	Mean Diameter (nm)	PDI	ξ Potential (mv)
1	0.005	0.50	50	3	38.4±2.4	161.1±4.2	0.167-0.211	-23.9±1.1
2	0.010	0.50	50	3	81.3±0.8	149.4±2.3	0.177-0.206	-22.5±1.5
3	0.015	0.50	50	3	52.3±1.5	141.6±3.1	0.204-0.225	-29.0±0.9
4	0.010	1.00	50	3	55.5±1.1	145.1±4.5	0.134-0.184	-33.9±1.1
5	0.010	0.25	50	3	31.8±1.7	163.7±3.8	0.083-0.147	-32.7±0.8
6	0.010	0.50	25	3	60.4±2.9	132.6±4.0	0.084-0.117	-55.9±2.2
7	0.010	0.50	75	3	96.6±0.4	152.1±2.9	0.177-0.235	-31.0±1.4
8	0.010	0.50	50	1	73.6±2.5	167.8±4.6	0.123-0.224	-32.8±1.2
9	0.010	0.50	50	4	97.8±0.6	150.2±5.1	0.109-0.156	-21.0±1.2

a. HPAE-co-PLA7:1 was used as an example.

b. Con. represents concentration, and PDI represents polydispersity index.

Table 5. The Influence of Fabricating Factors on EE and Particle Size by NP Method [a,b]

No.	BSA Con. (mg/ml)	Polymer Weight (mg)	EE (%)	Mean Diameter (nm)	PDI	ξ Potential (mv)
1	0.25	50	28.1±1.4	152.9±2.2	0.049-0.112	-30.5±2.4
2	0.5	50	59.8±2.5	146.8±1.4	0.087-0.134	-23.3±1.3
3	0.75	50	55.7±0.9	120.9±3.1	0.087-0.125	-20.3±1.5
4	0.5	25	53.8±1.2	158.1±4.6	0.117-0.221	-19.2±0.9
5	0.5	75	61.4±0.8	173.4±3.3	0.096-0.155	-24.3±1.1

a. HPAE-co-PLA7:1 was used as an example.

b. Con. represents concentration, and PDI represents polydispersity index.

increased viscosity of the formulation at the higher concentration of PVA 3% (w/v), the decrease in NP size was very small. The similar result was reported by previous paper [31]. BSA EE% was increasing with the increase of the concentration of PVA. The reason was that tight surface was formed from PVA macromolecules of high concentration, which increased diffusion resistance of BSA from the internal aqueous phase and stabilized the emulsion.

3.4.2.2. NP Method

NP method was a relative mild technique as compared with DE method because sonicators were not used by NP method. This technique also allowed for the preparation of large quantities of NPs since sonicators and homogenizers were not used in the process [32]. Briefly, NP technique was to precipitate the NPs through the use of an organic solvent that was entirely miscible with water. The formation of NPs with NP method could be carried out without any surfactant due to the amphiphilic properties of copolymers. Both the particle size and EE increase with the increase of copolymer concentration in acetone. While the EE increased first and then decreased with the increase of BSA concentration. These could be explained as mentioned in above sections. The particular results were listed in Table **5**.

The above data showed that the fabrication method had a significant effect on the EE. NPs with EE of 31.8–97.8% could be prepared by using DE method. Meanwhile, NPs with EE of 28.1–61.4% could be fabricated by using NP method at various conditions. The structure of HPAE-OHs4 hyperbranched moiety may be in favor of EE enhancement.

The structure preservation of BSA was also considered during its nanoencapsulation. Blending acetone in the organic phase with methylene chloride probably limited the contact between methylene chloride and BSA as well as reduced the surface tension between the organic phase and the water. The presence of acetone allowed NPs to solidify as a result of its solubility into water [33]. In addition, proteins are heat-sensitive and sonication is an exothermic operation. Therefore, the ice bath was used during primary emulsion.

Other experimental technique should be paid attention to during encapsulation. A rotation evaporator was used to reduce the evaporation time to avoid the protein release during stirring at room temperature. Moreover, organic solvent must be evaporated completely since the remained organic solvent will cause caking during centrifugation [34].

3.5. Morphology

The morphology of the NPs was investigated by the transmission electron microscopy technique. Fig. (**6**) showed the TEM image of NPs. It could be confirmed that the NPs appeared to be fine spherical shapes and no aggregation or adhesion occurred among the NPs made by both NP and DE methods.

3.6. *In Vitro* Release of BSA

The release profiles of BSA from the HPAE-co-PLA nanoparticles comparing with PLA nanoparticles were investigated and displayed in Fig. (**7**). After the initial burst, BSA release profiles displayed a sustained fashion. This sustained release could result from diffusion of BSA into the polymer wall and the protein through polymer wall as well as the erosion of the polymers. In this paper, a higher and faster BSA release was observed for HPAE-co-PLA nanoparticles than those of PLA. The difference could be relation to the presence of HPAE-OHs in PLA chains. There could be more protein molecules close to HPAE-co-PLA nanoparticles surface including those inserted among HPAE-OHs hyperbranched moiety on the surface of nanoparticles, which also would be much faster released. In all of the curves a burst effect was observed and a slow continuous release phase was followed. The maximal released amount is 82.13% for DE method and 91.28% for NP method in HPAE-co-PLA nanoparticles, respectively.

It was noticed that different fabrication methods led to various release behavior. The released amount and rate of BSA from NPs with NP method was much faster than that of DE method. The same result was also showed as previously reported [35]. When the polymers are not soluble in water, drug molecules dissolved in water may be very close to the outer NPs surface, forming a layer of molecules, susceptible to be easily and rapidly released. In addition, more burst release was observed from NPs fabricated with NP technique than those from DE method. This was because different methods led to various distributions of BSA molecules in the NPs. The fabrication method determined the amount of protein existing near the surface of NPs. Using DE method, most BSA molecules were encapsulated within the NPs as the multi-nanoreservoir systems. Using NP method, NPs

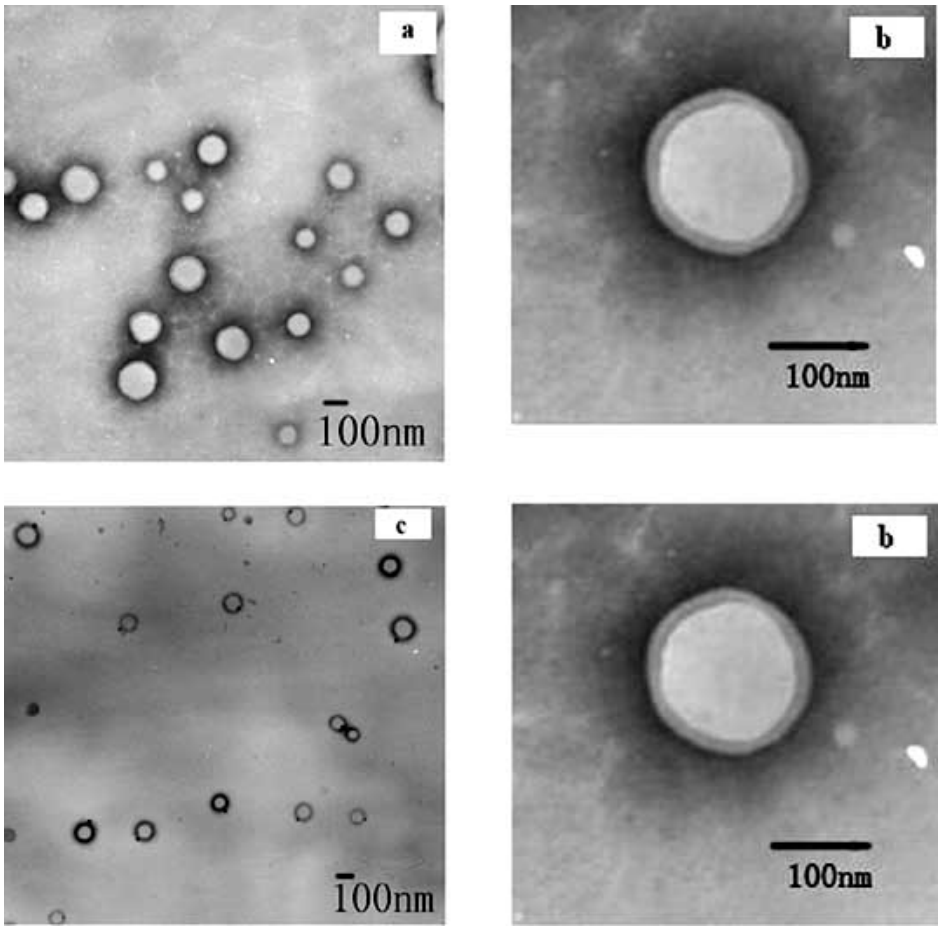

Fig. (6). TEM images and magnified images of BSA-loaded HPAE-co-PLA NPs fabrication by DE (a,b) and NP(c,d).

were formed as the multi-molecular polymeric micelles trapping BSA molecules near their outer layers.

3.7. Stability of BSA Released from NPs

Both direct and indirect methods could be employed to detect the BSA stability in the nanoparticles. In the direct method as described by Zhu *et al*. [36], the hydrophobic polymers in the nanoparticles was dissolved in acetone and the remained pellet of insoluble BSA was measured to obtain the total stability of BSA molecules including the releasable and non-releasable BSA molecules in the nanoparticles. In the indirect method as mentioned in the experiment part,

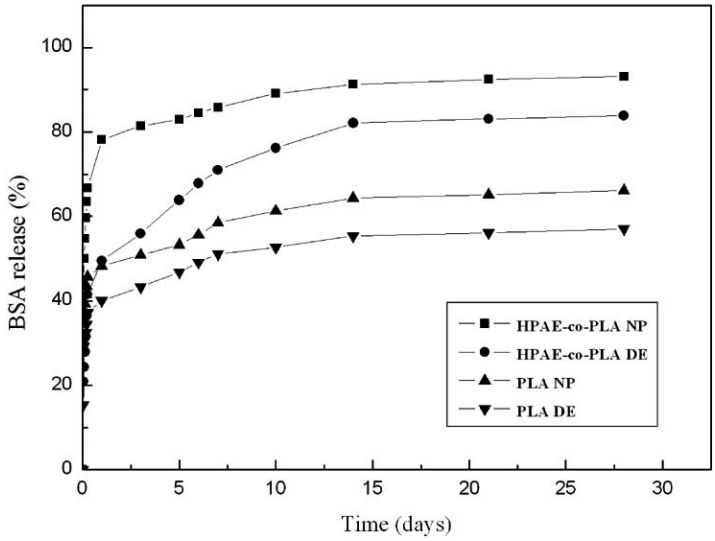

Fig. (7). *In vitro* release profiles of BSA from the PLA (Mw=48kDa) and HPAE-co-PLA (7:1) nanoparticles.

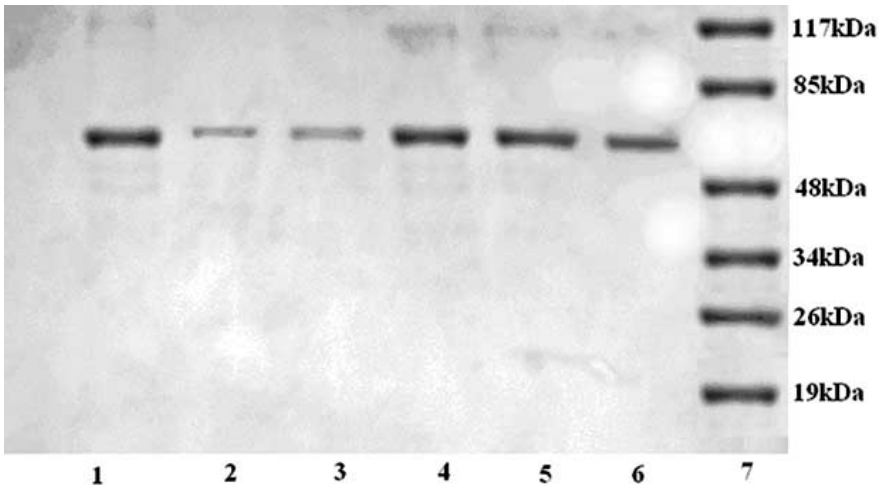

Fig. (8). SDS-PAGE results of BSA released from the nanoparticles after 14 days in PBS. Lane 1, BSA standard; lane 2, BSA released from nanoparticles of NP; lane 3, (DE); lane 4, BSA standard; lane 5, NP after 28 days; lane 6, DE after 28days; lane 7, MW standard.

only the released BSA from the nanoparticles was detected. In terms of practical application of protein delivery system in clinic, the data from the indirect method was more valuable to evaluate effectiveness of a protein delivery system. So the indirect method was used in our laboratory. The SDS-PAGE results of BSA released from nanoparticles after 14, 28 days are shown in Fig. (**8**). The non-reducing conditions employed for this analysis will preserve all aggregates linked by disulfide bonds [37]. Neither degradation nor soluble aggregation take place with the HPAE-co-PLA nanoparticles fabricated by both methods, suggesting that the HPAE moiety attributes to the preservation of BSA integrity. Many factors such as exposure of a protein to organic solvents, high temperature and shearing strength could make a protein deactivated during an encapsulation process [33]. Otherwise, the deleterious micro-environmental factors for the protein stability in the polymeric nanoparticles were acidic pH and the hydrophobic polymer surface [38]. To preserve BSA activity during its encapsulation, more moderate condition was employed such as acetone as water miscible solvent [39], sonication in an ice bath and ultracentrifugation at a low temperature as well as the use of the mechanical forces as low as possible. $Mg(OH)_2$ was successfully used to increase the microenvironmental pH and to prevent BSA from structural loss and aggregation for over one month [38,40]. The HPAE moiety possessed many hydrophilic hydroxyl groups that could form hydrogen bonds with the BSA molecule. An adaptive microenvironment for BSA was constructed from the polymer with hydrophilic hydroxyl groups to keep BSA stable. So the BSA activity could be preserved in the HPAE co-PLA nanoparticles.

Circular dichroism spectroscopy is a common method to analyze the secondary structure of a protein with high reliability. In the CD spectrum of the native BSA in PBS (pH 7.4), there were two extreme valleys at 208 and 222 nm [41]. The CD spectra of the free BSA in the supernatant from the release test after 28 days was measured and shown in Fig. (**9a**). Obviously, two extreme valleys at 208 and 222 nm occurred without any significant difference from those of the native BSA. The result indicated that the released BSA remained its original structure. The intensities of the double minimums reflected the helicity of BSA as more than 50% of α-helical structure. The declined intensity of the double minimums implied that the extent of α-helicity of the protein decreased. Because NP method fabricated nanoparticles in a more mild way, as for the HPAE-co-PLA nanoparticles, the secondary structure of the released BSA from the nanoparticles fabricated by the NP method remained more stable than by DE method. Compared to the CD spectrum of native BSA, the CD spectrum of the supernatant BSA released from the HPAE-co-PLA nanoparticles conformed more than that of BSA released from the PLA nanoparticles, indicating that the secondary structure of BSA released from HPAE-co-PLA nanoparticles was kept more stable than that from the PLA nanoparticles. The HPAE-co-PLA nanoparticles of a protein might be promising as a nasal delivery system, because the biological response of proteins encapsulated in some biodegradable nanoparticles was significantly greater than those in the microparticles when administered intranasally [42].

Meanwhile, fluorescence spectrum has been further used as a sensitive detector for the conformational change studies in the tertiary structures, as shown in Fig. (**9b**). The fluorescence emission spectrum of BSA at an excitation of 285 nm showed at 349 nm. Likewise, tertiary structure of BSA was also similar to BSA controlled.

CONCLUSION

A series of hyperbranched copolymers of HPAE–co-PLA were synthesized. Conjugating of PLA to HPAE-OHs was proved to be an available method for the fabrication preparation of NPs for protein delivery with following promising properties: the modification of hydrophobicity of PLA, the enhancement of EE and the structural stability of BSA released from the NPs. Besides the copolymer composition, fabrication methods (DE and NP methods) had significant influence on particle size, EE and release profile. Furthermore, a comprehensive investigating of the physicochemical characteristics (FT-IR, ^{1}H-NMR, TGA and DSC) of hyperbranched copolymer and their NPs aid in the design of new

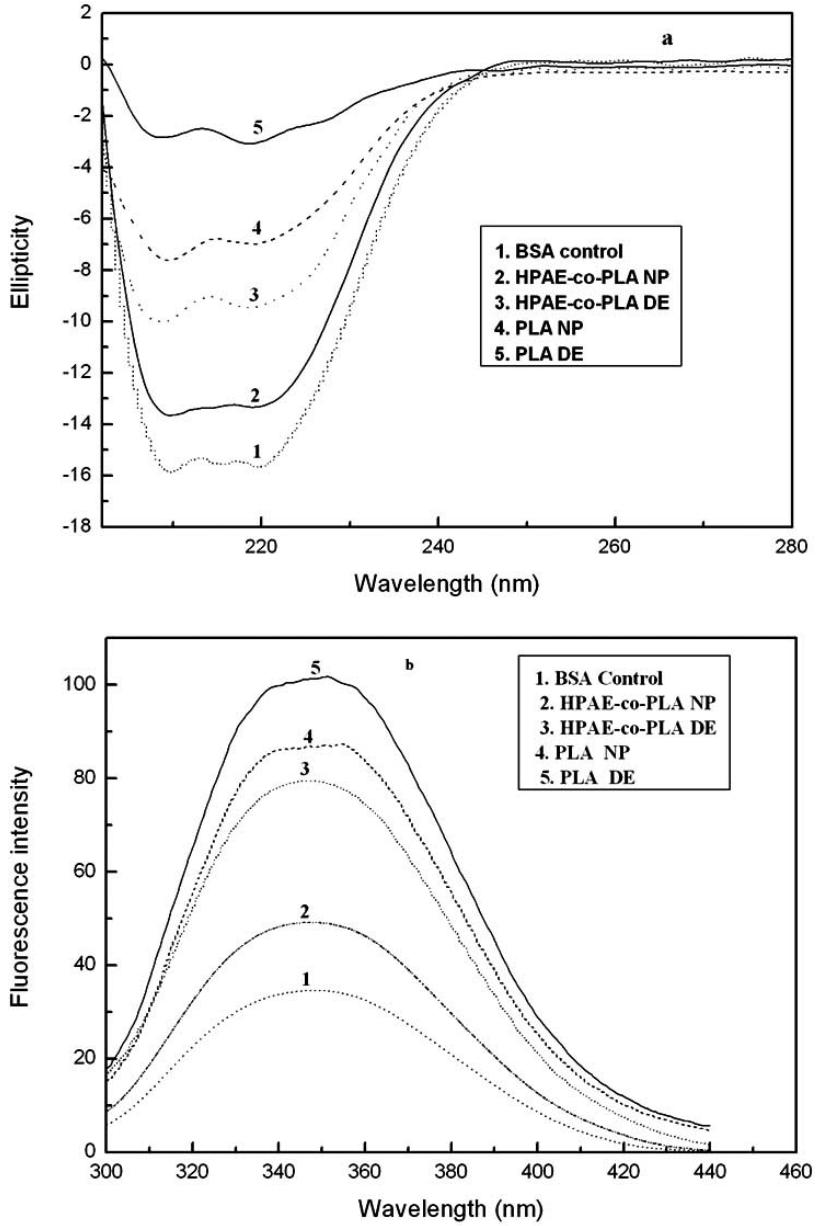

Fig. (9). The CD spectra (a) and the fluorescence spectra (b) of BSA released 28 days from NPs fabricated by DE and NP methods (HPAE-co-PLA (7:1), PLA (Mw=48kDa)).

amphiphilic copolymers and could help rationalize their *in vitro* performance.

ACKNOWLEDGEMENTS

Project supported by the National High Technology Research and Development Program of China (863) (No: 2006AA03Z321); the major program for fundamental research of the Chinese academy of sciences, China (No: KJCX2-YW-M02); the State Key Development Program for Basic Research of China (973) (No: 2009CB930200; 2010 CB934004).

REFERENCES

[1] Leo, E.; Ruozi, B.; Tosi, G.;Vandelli, MA. PLA-microparticles formulated by means a thermoreversible gel able to modify protein encapsulation and release without being co-encapsulated. *Int. J. Pharm.,* **2006***, 323*, 131-38.

[2] Gref, R.; Rodrigues, J.; Couvreur, P. Polysaccharides grafted with polyesters: novel amphiphilic copolymers for biomedical applications. *Macromolecules*, **2002**, *35*, 9861- 9867.

[3] Liu, M.; Zhou, Z.M.; Wang, X.F.; Xu, J.; Yang, K.; Cui, Q.; Chen, X.; Cao, M.Y.; Weng, J.; Zhang, Q.Q. Formation of poly (L, D-lactide) spheres with controlled size by direct dialysis. *Polymer*, **2007**, *48*, 5767-79.

[4] Liu, Y.; Zhao, Z.; Wei, J.; Ghzaoui, A.E.; Li, S.M. Micelles formed by self-assembling of polylactide/poly(ethylene glycol) block copolymers in aqueous solutions. *J. Colloid Interface Sci.*, **2007**, *314*, 470-77.

[5] Yuancai, D.; Si-Shen, F. *In vitro* and *in vivo* evaluation of methoxy polyethylene glycol-polylactide(MPEG-PLA) nanoparticles for small-molecule drug chemotherapy. *Biomaterials*, **2007**, *28*, 4154-60.

[6] Choi, S.W.; Kim, J.H: J. Design of surface-modified poly (D, L-lactide-co-glycolide) nanoparticles for targeted drug delivery to bone. *J. Control. Release*, **2007**, *122*, 24-30.

[7] Takami, A.; Masanori, B.; Mitsuru, A. Preparation of nanoparticles by the self-organization of polymers consisting of hydrophobic and

hydrophilic segments: Potential applications. *Polymer*, **2007**, *48*, 6729-47.

[8] Bikiaris, D.N.; Karayannidis, G.P. Synthesis and characterization of branched and partially crosslinked poly(ethylene terephthalate). *Polym Int.,* **2003**, *52*, 1230-39.

[9] Gao, C.; Yan, D: Hyperbranched polymers: from synthesis to applications. *Prog. Polym. Sci.*, **2004**, *29*, 183-275.

[10] McKee, M.G.; Unal, S.; Wilkes, G.L.; Long, T.E. Branched polyesters: recent advances in synthesis and performance. *Prog. Polym. Sci.,* **2005**, *30*, 507-39.

[11] Aulenta, F.; Hayes, W.; Rannard, S. Dendrimers: a new class of nanoscopic containers and delivery devices. *Eur. Polym. J.,* **2003**, *39*, 1741-71.

[12] Shcharbin, D.; Mazur, J.; Szwedzka, M.; Wasiak, M.; Palecz, B.; Przybyszewska, M.; Zaborski, M.; Bryszewska, M. Interaction between PAMAM 4.5 dendrimer, cadmium and bovine serum albumin: A study using equilibrium dialysis, isothermal titration calorimetry, zeta-potential and fluorescence. *Colloids Surf. B: Biointerfaces,* **2007**, *58*, 286-89.

[13] Kaneko, Y.; Imai, Y.; Shirai, K.; Yamauchi, T.; Tsubokawa, N. Preparation and properties of hyperbranched poly(amidoamine) grafted onto a colloidal silica surface. *Colloids Surf. A: Physicochem. Eng. Aspects,* **2006**, *289*, 212-18.

[14] Sha, Y.W.; Shen, L.; Hong, X.Y. A divergent synthesis of new aliphatic poly(ester-amine) dendrimers bearing peripheral hydroxyl or acrylate groups. *Tetrahedron Lett.*, **2002**, *43*, 9417-19.

[15] Twyman, L.J.; King, A.S.H.; Burnett, J.; Martin, I.K. Synthesis of aromatic hyperbranched PAMAM polymers. *Tetrahedron Lett.*, **2004**, *45*, 433-35.

[16] Tian, H.Y.; Deng, C.; Lin, H.; Sun, J.R.; Deng, M.X.; Chen, X.S.; Jing, X.B. Biodegradable cationic PEG-PEI-PBLG hyperbranched block copolymer: synthesis and micelle characterization. *Biomaterials*, **2005**, *26*, 4209-17.

[17] Rajesh, K.K.; Muthiah, G.; Munia G.; Tanay G.; Donald, E.B.; Souvik, M.; Jayachandran, N. K. Blood compatibility of novel water soluble hyperbranched polyglycerol-based multivalent cationic polymers and their interaction with DNA. *Biomaterials*, **2006**, *27*, 5377-90.

[18] Hyun, J.K.; Min, S.K.; Joon, S.C.; Bo, H.K.; Jae, K.Y.; Kwan, K.; Jong-sang, P. Synthesis and characterization of poly (amino ester) for slow biodegradable gene delivery vector. *Bioorg. Med. Chem.*, **2007**, *15*, 1708-15.

[19] Lu, Y.; Lin, D.; Wei, H. Y.; Shi, W.F. Synthesis and characterization of hyperbranched poly (amine-ester). *Acta Polymer. Sin.*, **2000**, *4*, 411-14.

[20] Bao, C.Y.; Jin, M.; Lu, R.; Zhang, T.R.; Zhao, Y.Y. Hyperbranched poly(amine-ester) templates for the synthesis of Au nanoparticles. *Mater. Chem. Phys.*, **2003**, *82*, 812-17.

[21] Hyon, S.H.; Jamshidi, K.; Ikada, Y. Synthesis of polylactides with different molecular weights. *Biomaterials*, **1997**, *18*, 1503- 1508.

[22] Zhu, B.K.; Wei, X.Z.; Xiao, L.; Xu, Y.Y.; Geckeler, K. E. Preparation and properties of hyperbranched poly (amine-ester) films using acetal cross-linking units. *Polym. Int.*, **2006**, *55*, 63-70.

[23] Rodrigues, J.S.; Santos-Magalhaes, N.S.; Coelho, L.C.B.B.; Couvreur, P.; Ponchel, G.; Gref, R. Novel core(polyester)-shell(polysaccharide) nanoparticles: protein loading and surface modification with lectins. *J. Control. Release*, **2003**, *92*, 103-12.

[24] Govender, T.; Stolnik, S.; Garnett, M.C.; Illum, L.; Davis, S.S. PLGA nanoparticles prepared by nanoprecipitation: drug loading and release studies of a water soluble drug. *J. Control. Release*, **1999**, *57*, 171-85.

[25] Karayannidis, G.P.; Roupakias, C.P.;Bikiaris, D.N.; Achilias, D.S. Study of various catalysts in the synthesis of poly (propylene terephthalate) and mathematical modeling of the esterification reaction. *Polymer*, **2003**, *44*, 931-42.

[26] Riley, T.; Govender, T.; Stolnik, S.; Xiong, C.D.; Garnett, M.C.; Illum, L.; Davis, S.S. Colloidal stability and drug incorporation aspects of micellar-like PLA-PEG nanoparticles. *Colloids Surf., B Biointerfaces*, **1999**, *16*, 147-59.

[27] Yasugi, K.; Nagasaki, Y.; Kato, M. ; Kataoka, K. Preparation and characterization of polymer micelles from poly(ethylene glycol)-poly(d, l-lactide) block copolymers as potential drug carrier. *J. Control. Release*, **1999**, *62*, 89- 100.

[28] Sułkowska, A.; Bojko, B.; Rownicka, J.; Sułkowski, W. Competition of drugs to serum albumin in combination therapy. *Biopolymers*, **2004**, *74*, 256-62.

[29] Verrecchia, T.; Spenlehauer, G.; Bazile, D.V.; Murry-Brelier, A.; Archimbaud, Y.; Veillard, M. Non-stealth (poly(lactic acid/albumin)) and stealth (poly(lactic acidpolyethylene glycol)) nanoparticles as injectable drugs carriers. *J. Control. Release,* **1995**, *36*, 49-61.

[30] Lamprecht, A.; Ubrich, N.; Hombreiro Pe´rez, M.; Lehr, C.M.; Hoffman, M.; Maincent, P. Biodegradable monodispersed nanoparticles prepared by pressure homogenization-emulsification. *Int. J. Pharm*., **1999**, *184*, 97-105.

[31] Ferdous, A.J.; Stembridge, N.Y.; Singh, M. Role of monensin PLGA polymer nanoparticles and liposomes as potentiator of ricin A immunotoxins *in vitro*. *J. Control. Release*, **1998**, *50*, 71-78.

[32] Birnbaum, D.T.; Kosmala, J.D.; Brannon-Peppas, L. Optimization of preparation techniques for poly(lactic acid-co-glycolic acid) nanoparticles. *J. Nanopart. Res*., **2000**, *2*, 173-81.

[33] Zambaux, M.F.;Bonneaux, F.; Gref, R.; Dellacherie, E.;Vigneron, C. Protein C-loaded monomethoxypoly (ethyleneoxide)-poly(lactic acid) nanoparticles. *Int. J. Pharm*., **2001**, *212*, 1 - 9.

[34] Zambaux, M.F.; Bonneaux, F.; Gref, F.; Dellacherie, E.; Vigneron, C. MPEO-PLA nanoparticles: effect of mPEO content on some of their surface properties. *J. Biomed. Mater. Res*., **1999**, *44*, 109-115.

[35] Ubrich, N.; Bouillot, P.H.; Pellerin, C.; Hoffman, M.; Maincent, P.H. Preparation and characterization of propranolol hydrochloride nanoparticles: a comparative study. *J. Control. Release*, **2004**, *97*, 291-300.

[36] Zhu, G.Z.; Mallery, S.R.; Schwendeman, S.P. Stabilization of proteins encapsulated in injectable poly (lactide-co-glycolide). *Nat. Biotechnol*., **2000**, *18*, 52-7.

[37] Crotts, G.; Park, T.G. Stability and release of bovine serum albumin encapsulated within poly(d, l-lactide-co-glycolide) microparticles. *J. Control. Release*, **1997**, *44*, 123-34.

[38] Zhu, G.Z.; Mallery, S.R.; Schwendeman, S.P. Stabilization of proteins encapsulated in injectable poly (lactide-co-glycolide). *Nat. Biotechnol*., **2000**, *18*, 52-57.

[39] Kang, F.; Singh, J. Conformational stability of a model protein (bovine serum albumin) during primary emulsification process of PLGA microspheres synthesis. *Int. J. Pharm*., **2003**, *260*, 149-56.

[40] Shenderova, A.; Bruke, T.G.; Schwendeman, S.P. The acidic microclimate in poly(lactide-co-glycolide) microspheres stabilizes camptothecins. *Pharm. Res*., **1999**, *16*, 241-48.

[41] Molina, I.; Li, S.; Martinez, M.B.; Vert, M. Protein release from physically crosslinked hydrogels of the PLA/PEO/PLA triblock copolymer-type. *Biomaterials*, **2001**, *22*, 363-69.

[42] Jung, T.; Kamm, W.; Breitenbach, A.; Hungere, K.D. Hundt, E.; Kissel, T. Tetanus toxoid loaded nanoparticles from sulfobutylated poly (vivylalcohol)-graft-poly (lactide-co-glycolide): evaluation of antibody response after oral and nasal application in mice. *Pharm. Res*., **2001**, *18*, 352-60.

Received: 18 May, 2009 **Revised: 18 August, 2009** **Accepted: 19 August, 2009**